

The British University in Egypt

**BUE Scholar**

---

Pharmacy

Health Sciences

---

3-2023

## The potential off-target neuroprotective effect of sister gliflozins suggests their repurposing despite not crossing the blood–brain barrier: From bioanalytical assay in rats into theory genesis

Shereen Mowaka

*The British University in Egypt, shereen.hassib@bue.edu.eg*

Moataz S. Hendy

*The British University in Egypt*

Ehab F. Elkady

*Pharmaceutical Chemistry Department, Faculty of Pharmacy, Cairo University*

Asmaa El-Zaher

*Pharmaceutical Chemistry Department, Faculty of Pharmacy, Cairo University*

Bassam M. Ayoub

*The British University in Egypt*

Follow this and additional works at: <https://buescholar.bue.edu.eg/pharmacy>



Part of the [Chemical and Pharmacologic Phenomena Commons](#), [Other Analytical, Diagnostic and Therapeutic Techniques and Equipment Commons](#), and the [Other Chemicals and Drugs Commons](#)

---

### Recommended Citation

Mowaka, Shereen; Hendy, Moataz S.; Elkady, Ehab F.; El-Zaher, Asmaa; and Ayoub, Bassam M., "The potential off-target neuroprotective effect of sister gliflozins suggests their repurposing despite not crossing the blood–brain barrier: From bioanalytical assay in rats into theory genesis" (2023). *Pharmacy*. 668.

<https://buescholar.bue.edu.eg/pharmacy/668>

This Article is brought to you for free and open access by the Health Sciences at BUE Scholar. It has been accepted for inclusion in Pharmacy by an authorized administrator of BUE Scholar. For more information, please contact [bue.scholar@gmail.com](mailto:bue.scholar@gmail.com).



**The Potential Off-target Neuroprotective Effect of Sister Gliflozins suggest their Repurposing Despite not Crossing the Blood Brain Barrier: from Bioanalytical Assay in Rats into Theory Genesis**

Journal:	<i>Journal of Separation Science</i>
Manuscript ID	jssc.202200921.R2
Wiley - Manuscript type:	Original Paper
Date Submitted by the Author:	n/a
Complete List of Authors:	Hendy, Moataz; Faculty of pharmacy, The British University in Egypt, Chemistry Department. Mowaka, Shereen; faculty of pharmacy, British university in Egypt, Analytical Chemistry; faculty of pharmacy, Helwan university, Analytical chemistry Elkady, Ehab; Cairo University Faculty of Pharmacy, Pharmaceutical Chemistry Department El-Zaher , Asmaa; Cairo University Faculty of Pharmacy, Pharmaceutical Chemistry Department Ayoub , Bassam ; School of Arts and Sciences, Concordia University Irvine (CUI)
Keywords:	Dapagliflozin, Drug Repurposing, Gliflozins, Neuroprotective Antidiabetics

SCHOLARONE™  
Manuscripts

1  
2  
3  
4  
5  
6  
7  
8

1           **The Potential Off-target Neuroprotective Effect of Sister Gliflozins suggest their**  
2           **Repurposing Despite not Crossing the Blood Brain Barrier: from Bioanalytical Assay in**  
3           **Rats into Theory Genesis**

9           4    Moataz S. Hendy <sup>1,2</sup>, Shereen Mowaka <sup>1,2,3</sup>, Ehab F Elkady <sup>4, \*\*</sup>, Asmaa El-Zaher <sup>4</sup>, Bassam M.  
10           5    Ayoub <sup>1,5,\*</sup>

11  
12           6    <sup>1</sup> Pharmaceutical Chemistry Department, Faculty of Pharmacy, The British University in Egypt,  
13           7    El-Sherouk city, 11837, Cairo, Egypt.

14           8    <sup>2</sup> The Center for Drug Research and Development (CDRD), Faculty of Pharmacy, The British  
15           9    University in Egypt, El-Sherouk city, 11837, Cairo, Egypt.

16           10   <sup>3</sup> Analytical Chemistry Department, Faculty of Pharmacy, Helwan University, Ain Helwan, 11795,  
17           11   Cairo, Egypt.

18           12   <sup>4</sup> Pharmaceutical Chemistry Department, Faculty of Pharmacy, Cairo University, 11562, Cairo,  
19           13   Egypt.

20           14   <sup>5</sup> School of Arts and Sciences, Concordia University Irvine, 92612, Irvine, CA, USA.

21  
22  
23  
24  
25  
26  
27  
28  
29  
30

16    **\* Corresponding author,**

31    Associate Professor Bassam M. Ayoub, Ph.D. School of Arts and Sciences, Concordia University  
32    Irvine (CUI), 1530 Concordia West, Irvine, CA, 92612, USA. Visiting Scholar, The British  
33    University in Egypt, Suez Road, El Sherouk City, Cairo Governorate 11837. Fax: (+20226300010)  
34    **[bassam.ayoub@cui.edu](mailto:bassam.ayoub@cui.edu), [bassam.ayoub@bue.edu.eg](mailto:bassam.ayoub@bue.edu.eg)**

35  
36  
37  
38  
39

21    **\*\* Corresponding author,**

40    Professor Ehab Farouk Elkady, Ph.D. Pharmaceutical Chemistry Department, Faculty of  
41    Pharmacy. Cairo University, Kasr El-Aini St, Cairo, 11562, Egypt. Fax (+0223628426)  
42    **[ehab.elkady@pharma.cu.edu.eg](mailto:ehab.elkady@pharma.cu.edu.eg)**

43  
44  
45  
46  
47

26    **Non-Standard Abbreviations**

48    **(BBB)** Blood Brain Barrier - **(CANa)** Canagliflozin - **(DAPA)** Dapagliflozin - **(EMPA)**  
49    Empagliflozin - **(LBTF)** Ligand Based Target Fishing - **(hENT1)** human Equilibrative Nucleoside  
50    Transporter 1  
51

52  
53  
54

30    **Keywords**

55    Dapagliflozin - Drug Repurposing - Gliflozins – Neuroprotective Antidiabetics  
56  
57

**Abstract**

Gliflozins are successfully marketed antidiabetic agents with a reported neuroprotective effect, this study tests their blood-brain barrier crossing ability. Henceforward, a computational hypothesis interpreting their effects was reasonable after failure to cross into the brain. A chromatographic bioassay for Canagliflozin, Dapagliflozin, and Empagliflozin was developed, validated, and applied to the rat's plasma and rat's brain. HPLC method robustness was tested over two levels using Design of Experiment on MINITAB®. It's the first method for gliflozins' detection in rats' brain tissue. The method was applied on eighteen rats, six for each drug. Concentrations in plasma were determined but neither of them was detected in brain at the described chromatographic conditions. A computational study for the three drugs was endorsing two techniques. Firstly, Ligand Based Target Fishing reveals possible targets for gliflozins. They showed an ability to bind with human Equilibrative Nucleoside Transporter 1, a regulator of adenosine extracellularly. Secondly, a docking study was carried out on this protein receptor. Results showed perfect alignment with a minimum of one hydrogen bond. Dapagliflozin achieved the lowest energy score with two hocking hydrogen bonds. This is proposing gliflozins ability to regulate Equilibrative Nucleoside Transporter 1 receptors in peripheries, elevating the centrally acting neuroprotective adenosine.

## 1. Introduction

Diabetes Mellitus (DM) and loss of cognitive functions are in a consistently correlated interrelationship. The brain is the most important glucose-dependent organ, and all central cognitive functions are chiefly dependent on insulin: the up regulator of glucose [1]. Accordingly, DM central complications are considered the worst, notably with neurodegenerative impairment [2]. Persistent hyperglycemia leads to an increased incidence of vascular dementia which is common in older people with diabetes [3]. These dementia complications are not related to other metabolic abnormalities, as DM is solely responsible for these resultant cognitive dysfunctions [4] in addition to the known insulin-like growth factor (IGF) signaling mechanisms that are essential in the brain for maintaining synaptic plasticity, and functionality [5].

Controlling DM as a paved path to tackling neurodegeneration is a well-rooted growing belief [1]. Generally, most antidiabetic agents possess a central action either direct or indirect. Those direct-acting antidiabetics function by controlling blood glucose levels leading to adequate glucose supply to the brain. The others act indirectly by increasing central mediators such as gliptins (Dipeptide Peptidase 4 Inhibitors) leading to more incretins that can cross the blood-brain barrier (BBB) and exert central effects [6]. The first quest of this study is to evaluate the BBB crossing ability of three antidiabetics sodium-glucose linked transporter-2 (SGLT-2) inhibitors: Canagliflozin (CANA), Dapagliflozin (DAPA), and Empagliflozin (EMPA) using direct HPLC analysis. Besides, correlating their indirect effects as antidiabetics with their direct effects -if there are any- in the central neurons using computational analysis. This was achieved successfully by developing a new chromatographic bioanalytical method to detect them in rats' plasma and rats' brain homogenate, besides utilizing computational molecular studies searching for their possible other biological targets and executing an interesting molecular docking study.

Some studies showed that some other oral antidiabetics (like metformin & glibenclamide) have a neuroprotective property [7]. A major *Cardiovascular Diabetology* original investigation by Lin *et al* showed that one of SGLT-2 inhibitors, EMPA, ameliorated significantly cerebral superoxide and 8-OHdG - a marker of DNA oxidative damage - experimentally in mice. Moreover, this attenuation of cerebral oxidative stress was associated with reduction of cerebral NADPH oxidase subunit gp91 [8]. Likewise, consolidating this point; EMPA was capable of debilitating neurological defects in rats' model of induced ischemia. Furthermore, levels of hypoxia-inducible

1  
2  
3 89 factor 1 (HIF-1) and vascular endothelial growth factor A (VEGF-A) were increased, resulting in  
4  
5 90 decreasing caspase-3 levels. Overexpression of this protein – caspase-3 - plays several roles in  
6  
7 91 Alzheimer's disease pathogenesis involving amyloidosis, formation of neurofibrillary tangles, and  
8  
9 92 neuronal apoptosis [9].

10  
11 93 In another study adopting a scopolamine-induced memory loss model for rats; Arafa et al  
12  
13 94 observed the beneficial effect of CANA, which may be correlated with acetylcholinesterase  
14  
15 95 inhibition [10]. A contribution to understanding the role of EMPA in the brain, Hayden et al proved  
16  
17 96 its role in the prevention of neuroglia in diabetic mice [11]. Also exactly like the antidiabetic  
18  
19 97 gliptins, SGLT-2 inhibitors may lead to an increase in GLP-1 concentrations, that in turn can cross  
20  
21 98 the BBB. However, this came with no fine empirical proof that calculates elevations in GLP-1  
22  
23 99 levels [12].

24 100 The gliflozins' (SGLT-2 inhibitors) story has been combined over three centuries. Evoked  
25  
26 101 in 1835 when French chemists isolated Phlorizin as a bicyclic flavonoid from the bark of apple  
27  
28 102 trees. Afterward, in 1886 prominent scientists Josef von Mering and Oscar Minkowski reported its  
29  
30 103 blood glucose-lowering effect and presupposed that the action occurs in the kidneys. This natural  
31  
32 104 flavonoid -Phlorizin- is the progenitor of all contemporary SGLT-2 inhibitors, evinced 130 years  
33  
34 105 later. As once in the early sixties of the twentieth century Chan et al, concluded that Phlorizin  
35  
36 106 blocks glucose transport across the renal tubules. Then in 1972 Glossmann et al, developed unique  
37  
38 107 research on isolated kidney brush border membranes showing that Phlorizin competitively binds  
39  
40 108 with certain receptors in kidney tubules [13]. Those receptors are the same glucose cotransporters  
41  
42 109 proteins responsible for intestinal absorption of sugars. Ten years after, it was discovered by  
43  
44 110 American researchers at the national health institute, that there are differences in glucose transport  
45  
46 111 capacity along the rat kidney tubule: the proximal part of the tubule could absorb more glucose  
47  
48 112 more quickly than the distal part. This effect was attributed later to the presence of SGLT-2. This  
49  
50 113 is depicted in (Figure 1) accompanied by structures of the studied SGLT2 inhibitors.

51  
52 114 Over years of intensive and accelerated research more data was revealed, more attention  
53  
54 115 was acquired, and those proteins were of great potential to be a major drug target. The idea that  
55  
56 116 their inhibition will help, originates from the day they were discovered. They chiefly are the only  
57  
58 117 symporters involved in the co-transportation of glucose and sodium in the proximal convoluted  
59  
60 118 tubule of a nephron in diabetic patients.

1  
2  
3 119 Today in USA & Europe, there are three approved SGLT-2 inhibitors and currently  
4  
5 120 authorized as new DM second-line treatment; CANA, DAPA, and EMPA [20]. EMPA has been  
6  
7 121 marked as the one with the highest selectivity for SGLT-2 receptors. CANA and DAPA possess  
8  
9 122 some other clinically proven influence. CANA can reduce the chances of stroke and heart attack  
10  
11 123 with an overall decrease in death related to circulatory events in diabetic patients. Reports also,  
12  
13 124 indicate its effect to reduce glucotoxicity and notably improve both insulin sensitivity and beta-  
14  
15 125 cell functions. On the other hand, DAPA decreases the risk of hypoglycemic events and do prevent  
16  
17 126 any unwanted blood pressure drop [14].

18 127 Before developing the BBB crossing study for SGLT-2 inhibitors, reviewing literature was  
19  
20 128 mandatory for all the previously developed bioanalytical methods either in human plasma or rats'  
21  
22 129 plasma as described in (Table 1).

23  
24 130 The current investigation includes developing a novel HPLC method for SGLT-2  
25  
26 131 inhibitors' bioanalysis in rats' plasma & brain tissue to check their BBB crossing ability at the  
27  
28 132 time of  $C_{max}$ . Spiked samples of blank rats' plasma and rats' brain tissue (with each of the three  
29  
30 133 drugs: CANA, DAPA & EMPA, separately) were analyzed using the proposed LC method. Full-  
31  
32 134 validated calibration curves for each of the drugs were developed. Reasonable lower limits of  
33  
34 135 quantification (LLOQ) were determined as part of the precision and accuracy assessment for each  
35  
36 136 calibration range and considered the lowest measured concentration in the matrix with acceptable  
37  
38 137 accuracy and precision. Successively, the method was effectively applied in concentration  
39  
40 138 quantifications within the biological matrices.

41  
42 139 Meanwhile, searching for biological clues explaining how and why gliflozins possess this  
43  
44 140 reported poly-pharmacology and neuroprotective effect. Two techniques of computational analysis  
45  
46 141 were approached. Firstly, in-silico Ligand-Based Target Fishing (LBTF), implementing (CANA-  
47  
48 142 DAPA-EMPA) each time as the query. This is based on 3D and 2D structure similarity search;  
49  
50 143 between the selected query drug and target annotated compound database. The second technique  
51  
52 144 was to proceed with docking in which the most prominent repeated target receptor acquired from  
53  
54 145 target fishing would be docked with gliflozins compound data base including the three investigated  
55  
56 146 CANA, DAPA and EMPA [36].  
57  
58  
59  
60

1  
2  
3 147 The results of chromatography study, testing ability of the drugs to pass the BBB along  
4  
5 148 with the computational study would contribute to providing optimal illustration about how these  
6  
7 149 drugs might work off their prescribed targets

## 8 9 150 **2. Methodology**

### 10 11 151 **2. 1. HPLC bioanalytical method & BBB crossing study**

#### 12 13 14 152 **Instruments**

15  
16 153 Thermo Fisher Scientific (Massachusetts, USA) UPLC-DAD of a model Ultimate 3000  
17  
18 154 was implemented using a Hypersil<sup>®</sup> C<sub>18</sub> column (100 × 3 mm, 3 μm). Christ<sup>®</sup> vacuum evaporator  
19  
20 155 (Germany), Acculab<sup>®</sup> vortex (NY, USA) and Centurion<sup>®</sup> centrifuge (Sussex, UK) were used for  
21  
22 156 the bioanalytical method.

#### 23 24 157 **Chemicals, reagents & biological samples**

25  
26 158 EMPA, CANA, and DAPA (purity 99.0% ± 1.0), rats' plasma, and rats' brain homogenate  
27  
28 159 were thankfully donated by the Center for Drug Research & Development CDRD (Research entity  
29  
30 160 in faculty of pharmacy the British University in Egypt) based on previous collaborations and  
31  
32 161 research grants. Other HPLC-grade Chemicals (methanol, acetonitrile, potassium dihydrogen  
33  
34 162 phosphate, tertiary butyl ethyl ether, and ethyl acetate were purchased from Fisher Scientific  
35  
36 163 (Loughborough, Leicestershire, UK). Ultra-pure deionized water was provided in-house. Blood  
37  
38 164 samples from Sprague Dawley rats of average weight 170-200 g were withdrawn (by CDRD) and  
39  
40 165 centrifuged at 2000 RPM for 20 minutes to acquire plasma. While rats' brain was extracted (by  
41  
42 166 CDRD animal facility), weighed, and homogenized over mortar with pestle via liquid nitrogen.  
43  
44 167 Then this brain homogenate was diluted to the tenth, weight/volume with saline before vigorous  
45  
46 168 vortex for 5 minutes.

47  
48 169 The work on animals was ethically approved by the Ethical Committee of the Faculty of  
49  
50 170 Pharmacy, the British University in Egypt, (Approval Number *Ex-2202*). Besides, all the  
51  
52 171 contributing researchers in this study are confirming that all experiments were performed in  
53  
54 172 accordance with relevant guidelines and regulations of the ethical committee in charge.  
55  
56 173 Additionally, all experiments involving animals complied with ARRIVE (Animal Research:  
57  
58 174 Reporting of *In Vivo* Experiments) recommended set of guidelines.



### 175 **Conditions of the Chromatographic bioassay**

176 The aim of the bioassay was to develop a highly robust technique considering the  
177 importance of method supremacy versus complicated matrices of plasma and brain homogenate.  
178 The adopted mobile phase was a complex of acetonitrile and methanol with 0.05 M concentration  
179 of phosphate buffer in a v/v/v mixture in ratios of (1:1:2) respectively. Phosphate buffer pH was  
180 adjusted to 3.5 by orthophosphoric acid. The pump flow rate was 1 mL/min delivering the optimum  
181 peak resolution while the injection volume was 10  $\mu$ L. BDS Hypersil® C18 column with  
182 dimensions (100 mm  $\times$  3 mm, 3  $\mu$ m) was utilized, prompting optimal detection, where the column  
183 temperature was set stable at 25  $^{\circ}$ C. The ultraviolet detector was set at 212 nm for CANA, and 225  
184 nm for both DAPA and EMPA.

### 185 **Biological Samples' extraction Framework**

186 Extraction was done for each 200  $\mu$ L rats' plasma or rats' brain tissue (after dilution of  
187 10%), where a calculated amount of every drug was added by spiking. Meanwhile, the mixture of  
188 the extracting solution made of ethyl acetate and tertiary butyl ethyl ether was prepared (1:1, v/v)  
189 and kept cold at -20  $^{\circ}$ C. From this mixture, 1.2 mL was withdrawn and have been added to each  
190 cold sample, sufficiently vortexed for 3 minutes then cooling centrifugation was performed for 15  
191 minutes at 12,000 RPM. Out of the clear upper supernatant, 1.0 mL was accurately withdrawn  
192 from each sample and then it was transferred into a labeled Eppendorf tube. These Eppendorf tubes  
193 were then transferred into the vacuum concentrator (70 min at 50  $^{\circ}$ C with 1000 RPM). After  
194 complete drying, reconstitution with a mixture of methanol and mobile phase (50:50, v/v), then  
195 3000 RPM vortex stirring was applied for 4 minutes subsequently to mixture addition.

### 196 **Setting Calibrations and Quality Control Samples**

197 For each drug, 2 mg/mL stock was prepared. Then, nine working solutions (100, 200, 300,  
198 400, 500, 600, 800, 850, and 1000  $\mu$ g/mL) were prepared in 10 mL volumetric flasks, completing  
199 to volume with methanol in all. After that, 10  $\mu$ L of each flask was added to blank plasma and  
200 brain samples (each 990  $\mu$ L). Subsequently, the obtained concentrations were 1, 2, 3, 4, 5, 6, 8,  
201 8.5, and 10  $\mu$ g/mL. Four concentrations were selected for Quality Control, which were 1  $\mu$ g/mL  
202 as LLOQ (Lower Limit of Quantitation), 3, 5, and 8.5  $\mu$ g/mL as "low, mid and high" Quality

203 Control samples. Each sample underwent the liquid-liquid extraction procedure aforementioned  
204 above.

### 205 **Bioanalytical Method Validation**

206 FDA bioanalytical method validation parameters were adopted and statistically computed  
207 [37]. Linearity calculations and calibrations were computed using each peak area. Overall  
208 precision (inter-day and intra-day) was studied through the calculation of RSD% for 5 replicates  
209 (n=5) that were determined for each quality control (QC) concentration. Accuracy for four QC  
210 samples (LLOQ - LOQ - MOQ - HOQ) was quantified expecting no deviation range of more than  
211 15%. Also, extraction recovery was determined by comparing the results of the extracted samples  
212 with post-extracted plasma samples possessing the same concentration. The matrix effect as a  
213 validation parameter was determined by comparing the peak area of the post-extracted sample with  
214 the equivalent neat sample. The last validation step was testing the stability of the QC samples, in  
215 which assessments were dependent on comparing the mean percent recovery of samples stored  
216 and those prepared freshly before injection with the same concentration. The accepted deviation  
217 degree is ( $\pm 15\%$ ) from the optimal concentration except for the LLOQ ( $\pm 20\%$ ). Testing stability:  
218 four different conditions were implemented which are: (1) short-term stability referring to  
219 analyzing QC samples after being kept for 6 hours at room temperature. (2) Freeze and thaw: that  
220 are testing samples after three cycles of  $-20\text{ }^{\circ}\text{C}$  overnight freezing then putting them to thaw for  
221 over 2 hours. (3) Postoperative stability where QC samples are kept in UPLC autosampler at a  
222 maintained temperature of  $25\text{ }^{\circ}\text{C}$  for a period of 24 hours. (4) Long-term stability testing after 15  
223 days of storage in a  $-80\text{ }^{\circ}\text{C}$  freezer.

### 224 **In Vivo Application & the BBB crossing study**

225 The BBB study was implemented using eighteen (n=6) adult male Sprague Dawley rats,  
226 six for each drug (weight range 140–180 g and age range 5-8 weeks). They were divided into  
227 groups of three one for each drug. Each group was housed in a plastic cage under controlled  
228 temperature ( $22 \pm 2\text{ }^{\circ}\text{C}$ ) and 12/12-h dark/light cycle with free access to rat chow and water.

229 CANA, DAPA, and EMPA were then orally administrated to each rat according to the  
230 group, and to ensure the animal survival within the experiment, the doses were assessed according  
231 to metabolic conversions from humans to animals. They were calculated after an intensive analysis

232 of human doses in the marketed tablets and those tried in clinical studies, plus the recently reported  
233 rat doses in literature. So, it differs from each drug to the other as follows: 20 mg/kg, 5 mg/kg, and  
234 10 mg/kg for CANA, DAPA, and EMPA; respectively. Then animals were sacrificed according to  
235 the reported  $T_{max}$ , 2 hours for CANA and EMPA [23] and 1.5 hours for DAPA [38]. Both plasma  
236 and brain samples were subjected to extraction before applying the proposed chromatographic  
237 method (*section 2. 1. HPLC bioanalytical method & BBB crossing study*).

## 238 2. 2. Computational analysis

239 The notorious multi-pharmacological effects of SGLT-2 inhibitors put roots for their  
240 repositioning. In other words, their characteristic clinical features made their possible usage in  
241 diseases rather than DM. Searching for possible biological targets is a complicated long pursuit.  
242 However, the most recently established bio-/chemo-informatics methodologies are providing  
243 efficient support in concluding the most probable target proteins. In this study, in-silico techniques  
244 were able to curtail time and effort. Two computational techniques were utilized in this proposed  
245 work. Ligand Base Target Fishing (LBTF) in which structure similarity search is carried out  
246 between the three drugs and a database of ligands. This technique is reported to be of a wide impact  
247 and is highly adequate in hunting accurate targets. The used tool here is SwissTargetPrediction  
248 available online <http://www.swisstargetprediction.ch/>. This is an online free platform provided by  
249 The Molecular Modelling group of the University of Lausanne, Switzerland. The adapted structure  
250 similarity principle portrays that similar compound molecules are prone to acquire similar  
251 properties.

252 Moreover, in SwissTargetPrediction, it is statistically quantified that similar biologically  
253 active molecules are likely to share their target receptors. This estimated quantification validates  
254 the authenticity of the “Molecular Similarity Hypothesis” putting forward that ‘similar molecules  
255 target common proteins’ [39]. Subsequently, each of CANA, DAPA, and EMPA was drowned and  
256 then used as a query molecule to search among a set of 376,342 actives of defined target receptors  
257 (3068 macromolecular targets) (Figure 2). The resultant predicted targets are arranged according  
258 to the similarity with ligands through a score that combines 2D and 3D structure similarity with  
259 the most similar activity to the query drug. The resultant data for each drug was exported as a  
260 spread data sheet for future data analysis. The results of target fishing showed common targets  
261 with the highest scores directly after their original SGLT receptors. Two main targets were

1  
2  
3 262 detected for the three drugs: human Equilibrative Nucleoside Transporter 1 (hENT1) and  
4  
5 263 Adenosine A2A Receptor (A2AR).  
6

7 264 The second used computational approach was a molecular docking study in which all  
8  
9 265 SGLT-2 inhibitors including CANA, DAPA, and EMPA besides the other previously synthesized  
10  
11 266 gliflozins, were docked versus the crystal structure of (hENT1). This study was applied to predict  
12  
13 267 the possible binding pose beside the molecular interactions within target pocket amino acids. The  
14  
15 268 docking study included the co-crystallized ligand isolated from the protein structure. Starting with  
16  
17 269 Protein Data Bank, searching for a target, choosing the most recent with relatively higher  
18  
19 270 resolution, which was PDB ID [6OB6] for (hENT1) plus the co-crystallized ligand [6-{{(4-  
20  
21 271 nitrophenyl)methyl}sulfanyl}-9-beta-D-ribofuranosyl-9H-purine] for (hENT1) [40].  
22

23 272 Initially, gliflozins were drowned energy minimized via Open Babel [41] using MMFF94  
24  
25 273 forcefield. Then, utilizing OpenEye modules, ROCS for conformer generation, and Make Receptor  
26  
27 274 for protein preparation. Docking was carried out by the FRED module which docks ligands blindly  
28  
29 275 to predict all possible binding modes, and lastly VIDA for visualization of the results.  
30  
31 276 ChemGauss4 Scores of dockings were concluded besides possible structure protein interactions  
32  
33 277 for further analysis and examination. Docking poses and similarity-based target fishing  
34  
35 278 representation are shown in (Figure 2) [42-47].  
36

## 37 279 **Discussion**

### 38 280 **3. 1. Extraction novelty and chromatographic renovation**

39 281 The aim of the current work is to experimentally test the presence of SGLT-2 inhibitors in  
40  
41 282 rats' plasma and rats' brain tissue in order to check their ability to cross the BBB. A new  
42  
43 283 chromatographic method was developed, implementing the previously mentioned UPLC  
44  
45 284 instrumentation relying on UV detection (section 2.1 Conditions of the Chromatographic  
46  
47 285 bioassay). The method development included many trials to overcome the matrix's undesirable  
48  
49 286 interferences. Accordingly, extraction procedures were crucial to retrieve the drugs away from the  
50  
51 287 confusing matrix. Liquid-Liquid extraction was adopted [48]. Applying different types of solvents  
52  
53 288 such as methylene chloride, petroleum ether, n-hexanes, ethyl acetate, diethyl ether, and tertiary  
54  
55 289 butyl ethyl ether, in addition to different mixtures of them on cold biological samples. Finally,  
56  
57 290 after the preliminary investigations mentioned above, a mixture of tertiary butyl ethyl ether and  
58  
59  
60

1  
2  
3 291 ethyl acetate (1:1, v/v) was the mixture of choice that achieved the most optimal recoveries. The  
4  
5 292 final extraction conditions (as mentioned under section 2.1. Biological samples' extraction  
6  
7 293 framework) required longer vacuum periods during evaporation, hence samples were evaporated  
8  
9 294 for 70 minutes to attain superior dryness. Afterward, reconstitution with 50  $\mu$ L methanol and 50  
10  
11 295  $\mu$ L mobile phase then using 3000 RPM vortex for each sample was sufficient to dissolve the  
12  
13 296 residue prior to injection.

14 297 The aim of the described bioassay was to develop a highly robust technique considering  
15  
16 298 the importance of the method supremacy versus complicated matrices of plasma and brain  
17  
18 299 homogenate. During UPLC method development, two stationary phases were tried. C18  
19  
20 300 Hypersil® Gold column (50 mm $\times$ 2.1 mm, 1.9  $\mu$ m) was initially employed, however, it showed no  
21  
22 301 satisfactory results. That might be attributed to its shortness in length with small particle size. This  
23  
24 302 made it inconvenient to produce good resolution away from relatively polar early eluted  
25  
26 303 interferants. When using the C18 BDS Hypersil® column (100 mm  $\times$  3 mm, 3  $\mu$ m), preferable  
27  
28 304 assay results were achieved. The temperature within the column compartment was kept stable at  
29  
30 305 25  $^{\circ}$ C to maintain the method's reproducibility.

31 306 Different mobile phase mixtures were tried. Simple mobile phases consisting of methanol  
32  
33 307 or acetonitrile with acidified water (0.1 % orthophosphoric acid or acetic acid) were attempted,  
34  
35 308 but they failed to achieve optimum ionization balance between the three compounds (CANA,  
36  
37 309 DAPA, EMPA), and the interfering residual traces extracted from plasma or brain. Thenceforth,  
38  
39 310 more complicated mixtures were prepared by mixing freshly prepared phosphate buffers of two  
40  
41 311 concentrations (0.05 & 0.01 M) and different pHs ranged from 3 to 4.5 with either methanol or  
42  
43 312 acetonitrile. This pH range was optimum relative to each drug's pKa (CANA= 13.34, DAPA=  
44  
45 313 12.57, and EMPA= 12.57) to yield sufficient ionization. However, still, no optimum results were  
46  
47 314 obtained regarding peak resolution and symmetry. Lastly and decisively, a ternary mixture of water  
48  
49 315 phase phosphate buffer (0.05 M & pH 3.5) accompanied by an organic phase of acetonitrile and  
50  
51 316 methanol (2:1:1, v/v), could achieve the matchless maneuver with the optimal peak purity. (Figure  
52  
53 317 3) portrays combined chromatograms of the three drugs in rats' plasma and rats' brain tissue. The  
54  
55 318 pump flow rate was settled to be 1.0 mL/min delivering optimum peak resolution. An injection  
56  
57 319 volume of 10  $\mu$ L was enough to get a reasonable peak area. The ultraviolet detector was set up at  
58  
59 320 212 nm for CANA, and 225 for both DAPA and EMPA according to the maxima of each drug in  
60

1  
2  
3 321 absorption spectra, to guarantee minimal matrix interference for each detection. As well as,  
4 322 adopting 3D spectra over the dynamic range of detection (200-400) to distinguish each drug peak  
5  
6 323 apart from matrix interference. This proposed method was employed in the analysis of the spiked  
7  
8 324 samples of rats' brains and plasma prior to calibration curves' construction for each drug in each  
9  
10 325 matrix ranging from 1 to 10  $\mu\text{g/mL}$  then determination of plasma concentrations of the drugs while  
11  
12 326 application in rats.

### 13 14 327 **Application on Rats**

15  
16 328 Eighteen animals were categorized into three sets, six for each drug (CANA, DAPA,  
17  
18 329 EMPA). To ensure animal survival within the experiment, the orally administered doses were  
19  
20 330 assessed according to metabolic conversions from humans to animals [37]. They were calculated  
21  
22 331 after an intensive analysis of human doses in the marketed tablets and those tried in clinical studies,  
23  
24 332 plus the recently reported rat doses in literature. So, it differs from each drug to the other as follows:  
25  
26 333 20 mg/kg, 5 mg/kg, and 10 mg/kg for CANA, DAPA, and EMPA; respectively. Doses were  
27  
28 334 optimum, in the median among the marketed dose and clinical trials concentrations. CANA official  
29  
30 335 dose is either 100 mg or 300 mg with a wider range in human clinical studies from (50-1600 mg)  
31  
32 336 [49], DAPA dosage form contains concentrations of 5 mg and 10 mg and in clinical trials dose  
33  
34 337 concentrations were ranging from 0.1 – 500 mg [50] and for EMPA dosage form has 10 or 25 mg  
35  
36 338 concentration while in clinical trials concentrations ranged between 0.5 to 800 mg [51]. After the  
37  
38 339  $T_{\text{max}}$  mentioned for each drug, animals were all sacrificed, chipping in brain and plasma. The  
39  
40 340 proposed UPLC method was used to detect CANA, DAPA, and EMPA in both rats 'plasma and  
41  
42 341 rats' brain tissue. The extracted brain samples of the three drugs showed chromatograms like the  
43  
44 342 blank samples suggesting their inability to cross the BBB (Figure 1 in the Supporting Information)  
45  
46 343 even below the LLOQ as there are no peaks at all, at the specified retention times of the drugs  
47  
48 344 suggesting no BBB crossing based on the current limit of detection (LOD) capability.

### 49 345 **Validation of the Chromatographic Method**

50  
51 346 During the detection of each component at its specific lambda max, no cross-interference  
52  
53 347 between matrix residuals and peak signals was obtained. Comparing blank plasma chromatogram  
54  
55 348 and (LLOQ) peak for each component validated method specificity and selectivity. The current  
56  
57 349 method achieved a well-eluted linearity range between 1-10  $\mu\text{g/mL}$  for all drugs based on the  
58  
59 350 AUP of each drug in both rats' plasma and brain tissue.

1  
2  
3 351 QC samples were calculated and analyzed with  $\pm 15\%$  deviation in concentration  
4  
5 352 quantification. Accuracy and precision (both inter-day and intraday) results were shown following  
6  
7 353 RSD% and RE% (n=5) for each concentration. Matrix effect and extraction recovery were also  
8  
9 354 concluded. Although the matrix effect is required mainly in MS detection, we preferred to do it in  
10  
11 355 our study to assure the absence of interference of co-eluting matrix components. All these  
12  
13 356 validation results are summarized in (Table 2). Moreover, method capacity versus different stress  
14  
15 357 conditions mentioned before in section (2. 1. HPLC bioanalytical method & BBB crossing study)  
16  
17 358 were examined, showing accepted adequate results, which are found in (Table 1 in Supporting  
18  
19 359 Information).

20  
21 360 Robustness of the UPLC method, as one of the validation parameters, was tested over two  
22  
23 361 levels (& one center point) using Design of Experiment (DOE) applying both Pareto charts & Box  
24  
25 362 Behnken design using MINITAB® software (Table 2 & 3 in the Supporting Information). The  
26  
27 363 lower level is referred to as -1, 0 was the center point, and +1 was the higher level of estimation.  
28  
29 364 Three chromatographic influential parameters were chosen as the studied factors. Flow rates at  
30  
31 365 (0.9, 1, 1.1 mL/min), Buffer pHs at (3.4, 3.5, 3.6), and column temperatures at (20, 25, 30 °C) were  
32  
33 366 tested. The results were analyzed based on both the AUP and retention time output results. The  
34  
35 367 results showed no significant difference based on both the Pareto charts (Figures 2-4 in the  
36  
37 368 Supporting Information) and Response surface methodology (RSM) (Figures 5-10 in Supporting  
38  
39 369 Information). The clearest conclusion that confirmed the robustness was the resulting p-values of  
40  
41 370 more than 0.05 which were considered “statistically insignificant”.

### 39 371 **3. 2. Computational Target Analysis and Molecular Docking**

42  
43 372 Referring to (2. 2. Computational analysis) two integrated in-silico simulations were  
44  
45 373 carried out. LBTF: a general scan for the three investigated drugs to interact with the updated  
46  
47 374 targets database. Thereafter, Molecular Docking between them and the consequent most common  
48  
49 375 target

50  
51 376 The remarkable finding through target fishing analysis is the interrelation between CANA,  
52  
53 377 DAPA, and EMPA with adenosine, adenosine receptors, and transporters. As for the three, the  
54  
55 378 most common targets were human Equilibrative Nucleoside Transporter 1 (hENT1), Adenosine  
56  
57 379 Receptors (Adora A2A), and Adenosine Kinase (Adk). Chiefly, hENT1 and Adora A2A possess  
58  
59 380 an essential role in modulating adenosine across body organs and most importantly the brain.

1  
2  
3 381 Above all, the prevalent extracellular presence of adenosine is physiologically rational regulating  
4  
5 382 various biological functions. However, adenosine precise concentration extracellularly is  
6  
7 383 depending on the balance between its formation, transportation, and elimination. Where's, a  
8  
9 384 cascade of metabolic ATP ectonucleotidases interactions rules its extracellular upregulation and  
10  
11 385 some others suppose its direct release and passage through the cell membrane. On the other hand,  
12  
13 386 adenosine clearance is governed by Adk, with its high affinity to adenosine leading to major flux  
14  
15 387 into cells through plasma membrane-specified transporters. The importance of adenosine is  
16  
17 388 coming out due to its biological protective roles both in physiological and pathophysiological  
18  
19 389 conditions. Almost, all cell types possess at minimum one adenosine receptor subtype. This  
20  
21 390 illustrates its essential role regarding body organ protection and cell regeneration. This protective  
22  
23 391 biological function differs according to the site of action. It may act by increasing blood supply or  
24  
25 392 reducing inflammation leading to its cardioprotective, cerebroprotective, and neuroprotective  
26  
27 393 influences [52].

26 394 Both hENT1 and Adora A2A as molecular targets are widely distributed over human  
27  
28 395 organs, achieving their roles in the adenosine regulation cycle in and outside cells. ENT1 is  
29  
30 396 essential for controlling adenosine levels plus its role in nucleoside uptake for DNA and RNA  
31  
32 397 formation. Clinically ENT1 is a target for a class of medications namely adenosine reuptake  
33  
34 398 inhibitors. Those drugs are blocking the action of the nucleoside transporters, which in turn  
35  
36 399 upregulates adenosine outside cells boosting its extracellular clinical effects over its specified P1  
37  
38 400 receptors. These extracellular effects are discontinued when adenosine is driven back toward the  
39  
40 401 intracellular via ENTs. Normally, activation of A1, A2A, A2B, and A3 (P1 receptors) by forming  
41  
42 402 an active complex with adenosine cascades its inward transportation [53]. So, inhibition of this  
43  
44 403 reuptake would keep the levels of extracellular adenosine relatively adequate to enhance  
45  
46 404 neurotransmission signal cascades executing central neuroprotection effects. Most probably, this  
47  
48 405 is entirely facilitated through cAMP/p-CREB/Bcl2 signaling routes; it was found that activation  
49  
50 406 of cAMP-dependent protein kinase A(PKA) mediates localized inflammation responses and  
51  
52 407 interrupts neuronal cell apoptosis. In addition, ENT1 inhibition would directly improve cerebral  
53  
54 408 blood flow due to an increment in Nitric oxide (NO) production restoring neuroprotection. Also,  
55  
56 409 a previous study on ENT1 inhibition attributed its neuroprotective effect to the reduction in  
57  
58 410 glutamate neurotransmitters that govern neuronal excitability. To all intents and purposes, the  
59  
60 411 point is: antagonizing ENT1 would greatly affect the adenosine levels outside neurons fortifying



1  
2  
3 412 its neuroprotective impact [54]. Not only that, ENT1 knock-out mouse models were made to  
4 413 understand its pharmacological effect and portrayed outstanding elevated levels of systemic  
5 414 adenosine in plasma. These animal models are proven to acquire multiorgan protection, especially  
6 415 during ischemia and reperfusion hard times [55].  
7  
8  
9

10  
11 416 Molecular docking studies were implemented on the hENT1 receptor supposing that the  
12 417 interaction between database compounds (gliflozins) and the receptor target would be outside the  
13 418 brain. As they have not been able to pass BBB or even have previously reported having any utility  
14 419 to pass whether in human or in an animal study. Consequently, the study is aiming to elucidate and  
15 420 hypothesize how would gliflozins act as an adenosine reuptake receptor modulator in peripheral  
16 421 organs elevating adenosine levels in the plasma and leading to their neuroprotective central desired  
17 422 outcomes. In correspondence, Adora A2A is a direct receptor for adenosine regulation, but its role  
18 423 as neuroprotective depends on the adenosine concentration balance that is entirely achieved over  
19 424 central activation. On the other hand, Adora A2A peripheral activation gives rise to other  
20 425 cytoprotective signal cascades rather than central, such as being cardioprotective or  
21 426 fibroprotective.  
22  
23  
24  
25  
26  
27  
28  
29

30 427 Over the proceeding of the docking process, the co-crystallized ligand isolated with the  
31 428 protein was employed to figure out the physical parameters of the target site of action within  
32 429 protein amino acids prior to protein preparation. Subsequently, molecular docking calculations  
33 430 were simulated for the gliflozins database. Docking results showed that all gliflozins were in stable  
34 431 and optimal alignment inside the receptor molecular surface. According to energy scores, DAPA  
35 432 achieved the highest score while the ligand was the eighth. Low energy complexes between the  
36 433 compounds and binding pocket plus Hydrogen bond formation, consolidate the actual ability of  
37 434 those SGLT2 inhibitors to fit and act as ENT1 potential regulators. Moreover, they might inhibit  
38 435 adenosine reuptake, fulfilling the desired pharmacological neuroprotective outcomes. The three  
39 436 drugs: CANA, DAPA, and EMPA were having higher scores than the protein co-crystallized  
40 437 ligand, showing perfect similar orientation. DAPA was able to form two hydrogen bonds between  
41 438 its sugar moiety and two amino acids (Arginine 345 and Asparagine 407). Its perfect compact  
42 439 posture in the pocket validates the strength of the electrostatic interactions versus the surrounding  
43 440 amino acids. The ligand made one hydrogen bond with Glutamine 158 with its central purine  
44 441 moiety. OpenEye® energy scores are absolute values mimicking drug receptors' overall complex  
45  
46  
47  
48  
49  
50  
51  
52  
53  
54  
55  
56  
57  
58  
59  
60

1  
2  
3 442 energy, the lower the value the better is fitting. These scores are presented in (Table 3), also  
4 443 hydrogen bonds between DAPA/Ligand versus receptor are shown in (Figure 4)

#### 7 444 **Conclusion**

9  
10 445 The proposed UPLC method confirmed the inability of the studied drugs (CANA, DAPA &  
11 446 EMPA) to cross the BBB based on the rats' study that included eighteen animals after the ethical  
12 447 committee approval. The developed method will be beneficial for future bioanalytical studies  
13 448 especially because it is the first method that considered the quantification of the drugs in the rats'  
14 449 brain tissue. Moreover, it is the first unified method that is considered a direct estimation of all  
15 450 three gliflozins in rats' plasma. The developed extraction procedure was optimized to be valid for  
16 451 both the rats' plasma & brain tissue simultaneously based on a new mixture that had been used for  
17 452 the liquid-liquid extraction. The key for the computational study is that the three antidiabetic agents  
18 453 SGLT-2 inhibitors (CANA, DAPA, and EMPA) have a well-established neuroprotective clinical  
19 454 effect, recently considered, and assessed in the literature. LBTF structure similarity study was  
20 455 carried out using SwissTargetPredict, subsequent to biological literature analysis of the target  
21 456 fishing results. It was found that gliflozins have a considerable affinity toward ENT1 receptor  
22 457 which is crucial in adenosine extracellular concentration. A blind Molecular Docking study  
23 458 showed perfect alignment of the prepared database of all synthesized gliflozins with ENT1 crystal  
24 459 structure isolated with high-resolution. DAPA showed the highest score of binding with the lowest  
25 460 energy complex plus two hydrogen bond formations hocking the structure within the amino acids.  
26 461 This study proposes that an SGLT2 inhibitor might be capable of antagonizing ENT1 receptors in  
27 462 peripheral tissues resulting in a high concentration of adenosine in plasma, subsequently relative  
28 463 elevation in its concentration in the brain via its BBB transporters. These increments of the  
29 464 extracellular adenosine in brain compartments are the reason for the prominent cytoprotecting  
30 465 impacts with overall ameliorations in mind and cognitive functions.

#### 31 466 **Acknowledgements**

32 467 The authors are thankful to The Center for Drug Research and Development (CDRD) at the British  
33 468 University in Egypt for its support with rats and consumables. Special gratitude to Professor  
34 469 Mohey Elmarar, the dean of the Faculty of Pharmacy, for enhancing research constantly with all  
35 470 the required support and cooperation in CDRD. In addition, all authors have no conflict of interest  
36 471 of any kind to declare.

472 **References**

- 473 1. J.L. Milstein, H.A. Ferris, The brain as an insulin-sensitive metabolic organ, *Mol Metab.*  
474 (2021) 101234.
- 475 2. A.J. Scheen, Central nervous system: a conductor orchestrating metabolic regulations  
476 harmed by both hyperglycaemia and hypoglycaemia, *Diabetes Metab.* 36 (2010) S31–S38.
- 477 3. A.H. Abdelhafiz, E. McNicholas, A.J. Sinclair, Hypoglycemia, frailty and dementia in  
478 older people with diabetes: reciprocal relations and clinical implications, *J Diabetes*  
479 *Complications.* 30 (2016) 1548–1554.
- 480 4. K. Mattishent, Y.K. Loke, Bi-directional interaction between hypoglycaemia and cognitive  
481 impairment in elderly patients treated with glucose-lowering agents: A systematic review and  
482 meta-analysis, *Diabetes Obes Metab.* 18 (2016) 135–141. <https://doi.org/10.1111/dom.12587>.
- 483 5. J. Boucher, A. Kleinridders, C.R. Kahn, Insulin receptor signaling in normal and insulin-  
484 resistant states., *Cold Spring Harb Perspect Biol.* 6 (2014).  
485 <https://doi.org/10.1101/cshperspect.a009191>.
- 486 6. B.M. Ayoub, H.E. Michel, S. Mowaka, M.S. Hendy, M.M. Tadros, Repurposing of  
487 Omarigliptin as a Neuroprotective Agent Based on Docking with A2A Adenosine and AChE  
488 Receptors, Brain GLP-1 Response and Its Brain/Plasma Concentration Ratio after 28 Days  
489 Multiple Doses in Rats Using LC-MS/MS, *Molecules.* 26 (2021) 889.
- 490 7. F. Chen, R.R. Dong, K.L. Zhong, A. Ghosh, S.S. Tang, Y. Long, M. Hu, M.X. Miao, J.M.  
491 Liao, H.B. Sun, Antidiabetic drugs restore abnormal transport of amyloid- $\beta$  across the blood–brain  
492 barrier and memory impairment in db/db mice, *Neuropharmacology.* 101 (2016) 123–136.
- 493 8. B. Lin, N. Koibuchi, Y. Hasegawa, D. Sueta, K. Toyama, K. Uekawa, M. Ma, T.  
494 Nakagawa, H. Kusaka, S. Kim-Mitsuyama, Glycemic control with empagliflozin, a novel selective  
495 SGLT2 inhibitor, ameliorates cardiovascular injury and cognitive dysfunction in obese and type 2  
496 diabetic mice, *Cardiovasc Diabetol.* 13 (2014) 1–15.
- 497 9. A. Płóciennik, M. Predecki, E. Zuba, M. Siudzinski, J. Dorszewska, Activated caspase-3  
498 and neurodegeneration and synaptic plasticity in Alzheimer’s disease, *Adv Alzheimer Dis.* 4  
499 (2015) 63.
- 500 10. N.M.S. Arafa, E.H.A. Ali, M.K. Hassan, Canagliflozin prevents scopolamine-induced  
501 memory impairment in rats: Comparison with galantamine hydrobromide action, *Chem Biol*  
502 *Interact.* 277 (2017) 195–203.

- 1  
2  
3 503  
4  
5 504 11. M.R. Hayden, D.G. Grant, A.R. Aroor, V.G. DeMarco, Empagliflozin ameliorates type 2  
6  
7 505 diabetes-induced ultrastructural remodeling of the neurovascular unit and neuroglia in the female  
8  
9 506 db/db mouse, *Brain Sci.* 9 (2019) 57.
- 10 507 12. P. Millar, N. Pathak, V. Parthasarathy, A.J. Bjourson, M. O’Kane, V. Pathak, R.C. Moffett,  
11  
12 508 P.R. Flatt, V.A. Gault, Metabolic and neuroprotective effects of dapagliflozin and liraglutide in  
13  
14 509 diabetic mice, *Journal of Endocrinology.* 234 (2017) 255–267.
- 15 510 13. H. Glossmann, D.M. Neville Jr, Phlorizin receptors in isolated kidney brush border  
16  
17 511 membranes Differential enzymatic modification of high-affinity receptors and unspecific binding  
18  
19 512 sites, *Biochimica et Biophysica Acta (BBA)-Biomembranes.* 323 (1973) 408–414.
- 20 513 14. B.F. Mandell, SGLT-2 inhibitors are potential game-changers (for more than diabetes),  
21  
22 514 *Cleve Clin J Med.* 88 (2021) 588–589.
- 23  
24 515 15. M. Iqbal, E. Ezzeldin, K.A. Al-Rashood, Y.A. Asiri, N.L. Rezk, Rapid determination of  
25  
26 516 canagliflozin in rat plasma by UHPLC–MS/MS using negative ionization mode to avoid adduct-  
27  
28 517 ions formation, *Talanta.* 132 (2015) 29–36.
- 29 518 16. M. Iqbal, N.Y. Khalil, A.M. Alanazi, K.A. Al-Rashood, A simple and sensitive high  
30  
31 519 performance liquid chromatography assay with a fluorescence detector for determination of  
32  
33 520 canagliflozin in human plasma, *Analytical Methods.* 7 (2015) 3028–3035.
- 34 521 17. P.B. Dudhe, M.C. Kamble, RP-HPLC method development and validation for the  
35  
36 522 determination of canagliflozin in human plasma, *Int J Pharm Tech Res.* 9 (2016) 174–181.
- 37  
38 523 18. S. Kobuchi, K. Yano, Y. Ito, T. Sakaeda, A validated LC-MS/MS method for the  
39  
40 524 determination of canagliflozin, a sodium–glucose co-transporter 2 (SGLT-2) inhibitor, in a lower  
41  
42 525 volume of rat plasma: application to pharmacokinetic studies in rats, *Biomedical Chromatography.*  
43  
44 526 30 (2016) 1549–1555.
- 45 527 19. S. Dong, H. Niu, Y. Wu, J. Jiang, Y. Li, K. Jiang, X. Wang, M. Zhang, M. Han, S. Meng,  
46  
47 528 Plasma pharmacokinetic determination of canagliflozin and its metabolites in a type 2 diabetic rat  
48  
49 529 model by UPLC-MS/MS, *Molecules.* 23 (2018) 1229.
- 50 530 20. D. Mohamed, M.S. Elshahed, T. Nasr, N. Aboutaleb, O. Zakaria, Novel LC–MS/MS  
51  
52 531 method for analysis of metformin and canagliflozin in human plasma: application to a  
53  
54 532 pharmacokinetic study, *BMC Chem.* 13 (2019) 1–11.

- 1  
2  
3 533 21. M. Ramiseti, L.R. Atmakuri, B.R.M. Venkata, V. Adireddy, Simultaneous determination  
4 534 of canagliflozin and metformin in human plasma by LC-MS/MS assay and its application to a  
5 535 human pharmacokinetic study, *Ind J Pharm Educ Res.* 52 (2019) 364–372.
- 6  
7  
8 536 22. A.B. van der Aart-van, A.M.A. Wessels, H.J.L. Heerspink, D.J. Touw, Simple, fast and  
9 537 robust LC-MS/MS method for the simultaneous quantification of canagliflozin, dapagliflozin and  
10 538 empagliflozin in human plasma and urine, *Journal of Chromatography B.* 1152 (2020) 122257.
- 11  
12  
13 539 23. T. Wattamwar, A. Mungantiwar, S. Gujar, N. Pandita, Development of LC-MS/MS  
14 540 method for simultaneous determination of Canagliflozin and Metformin in human plasma and its  
15 541 pharmacokinetic application in Indian population under fast and fed conditions, *Journal of*  
16 542 *Chromatography B.* 1154 (2020) 122281.
- 17  
18  
19 543 24. P. Alam, M. Iqbal, A.I. Foudah, M.H. Alqarni, F. Shakeel, Quantitative determination of  
20 544 canagliflozin in human plasma samples using a validated HPTLC method and its application to a  
21 545 pharmacokinetic study in rats, *Biomedical Chromatography.* 34 (2020) 4929.
- 22  
23  
24 546 25. Emam RA, Emam AA. Ecofriendly appraisal of stability-indicating high-performance  
25 547 chromatographic assay of canagliflozin and metformin with their toxic impurities; in silico toxicity  
26 548 prediction, *Journal of Separation Science.* 25 (2022) 2200754.
- 27  
28  
29 549 26. A.-F. Aubry, H. Gu, R. Magnier, L. Morgan, X. Xu, M. Tirmenstein, B. Wang, Y. Deng,  
30 550 J. Cai, P. Couerbe, Validated LC–MS/MS methods for the determination of dapagliflozin, a  
31 551 sodium-glucose co-transporter 2 inhibitor in normal and ZDF rat plasma, *Bioanalysis.* 2 (2010)  
32 552 2001–2009.
- 33  
34  
35 553 27. S. Goday, A.R. Shaik, P. Avula, Development and validation of a LC-ESI-MS/MS based  
36 554 bioanalytical method for dapagliflozin and saxagliptin in human plasma, *Indian J Pharm Educ Res.*  
37 555 52 (2018) S277–S286.
- 38  
39  
40 556 28. S. Donepudi, S. Achanta, Simultaneous estimation of saxagliptin and dapagliflozin in  
41 557 human plasma by validated high performance liquid chromatography-ultraviolet method, *Turk J*  
42 558 *Pharm Sci.* 16 (2019) 227.
- 43  
44  
45 559 29. M.A. Omar, H.M. Ahmed, M.A. Abdel Hamid, H.A. Batakoushy, New spectrofluorimetric  
46 560 analysis of dapagliflozin after derivatization with NBD-Cl in human plasma using factorial design  
47 561 experiments, *Luminescence.* 34 (2019) 576–584.
- 48  
49  
50  
51  
52  
53  
54  
55  
56  
57  
58  
59  
60

- 1  
2  
3 562 30. A.A. El-Zaher, H.A. Hashem, E.F. Elkady, M.A. Allam, A validated LC-MS/MS  
4 563 bioanalytical method for the simultaneous determination of dapagliflozin or saxagliptin with  
5 564 metformin in human plasma, *Microchemical Journal*. 149 (2019) 104017.
- 6  
7  
8 565 31. N.S. Abbas, S.M. Derayea, M.A. Omar, G.A. Saleh, TLC-spectrodensitometric method for  
9 566 simultaneous determination of dapagliflozin and rosuvastatin in rabbit plasma: stability indicating  
10 567 assay and kinetic studies, *RSC Adv.* 10 (2020) 40795–40805.
- 11  
12  
13 568 32. S.A. Abdel-Gawad, O. Afzal, Spectrodensitometric and ultra-performance liquid  
14 569 chromatographic quantification of dapagliflozin and saxagliptin in their dosage form and human  
15 570 plasma, *Tropical Journal of Pharmaceutical Research*. 20 (2021) 1223–1231.
- 16  
17  
18 571 33. M.M. Mabrouk, S.M. Soliman, H.M. El-Agizy, F.R. Mansour, A UPLC/DAD method for  
19 572 simultaneous determination of empagliflozin and three related substances in spiked human plasma,  
20 573 *BMC Chem.* 13 (2019) 1–9.
- 21  
22  
23 574 34. P.A. Shah, P.S. Shrivastav, A. George, Mixed-mode solid phase extraction combined with  
24 575 LC-MS/MS for determination of empagliflozin and linagliptin in human plasma, *Microchemical*  
25 576 *Journal*. 145 (2019) 523–531.
- 26  
27  
28 577 35. M. Rizk, A.K. Attia, H.Y. Mohamed, M.S. Elshahed, Validated Voltammetric Method for  
29 578 the Simultaneous Determination of Anti-diabetic Drugs, Linagliptin and Empagliflozin in Bulk,  
30 579 *Pharmaceutical Dosage Forms and Biological Fluids, Electroanalysis*. 32 (2020) 1737–1753.
- 31  
32  
33 580 36. M.I. Ismail, S. Mohamady, N. Samir, K.A.M. Abouzid, Design, Synthesis, and Biological  
34 581 Evaluation of Novel 7 H-[1, 2, 4] Triazolo [3, 4-b][1, 3, 4] thiadiazine Inhibitors as Antitumor  
35 582 Agents, *ACS Omega*. 5 (2020) 20170–20186.
- 36  
37  
38 583 37. Food and Drug Administration, Guidance for industry: bioanalytical method validation,  
39 584 [Http://Www. Fda. Gov/Cder/Guidance/4252fnl. Pdf.](http://www.fda.gov/cder/guidance/4252fnl.pdf) (2001).
- 40  
41  
42 585 38. Aameeduzzafar, I. El-Bagory, N.K. Alruwaili, S.S. Imam, F.A. Alomar, M.H. Elkomy, N.  
43 586 Ahmad, M. Elmowafy, Quality by design (QbD) based development and validation of  
44 587 bioanalytical RP-HPLC method for dapagliflozin: Forced degradation and preclinical  
45 588 pharmacokinetic study, *J Liq Chromatogr Relat Technol*. 43 (2020) 53–65.
- 46  
47  
48 589 39. A. Daina, O. Michielin, V. Zoete, SwissTargetPrediction: updated data and new features  
49 590 for efficient prediction of protein targets of small molecules, *Nucleic Acids Res*. 47 (2019) W357–  
50 591 W364.
- 51  
52  
53  
54  
55 592

- 1  
2  
3 593 40. N.J. Wright, S.-Y. Lee, Structures of human ENT1 in complex with adenosine reuptake  
4 594 inhibitors, *Nat Struct Mol Biol.* 26 (2019) 599–606.
- 5 595 41. N.M. O’Boyle, M. Banck, C.A. James, C. Morley, T. Vandermeersch, G.R. Hutchison,  
6 596 Open Babel: An open chemical toolbox, *J Cheminform.* 3 (2011) 1–14.
- 7 597 42. OEDOCKING 3.4.0.2; OpenEye Scientific Software: Santa Fe, NM.  
8 598 <http://www.eyesopen.com.>, (n.d.).
- 9 599 43. ROCS 3.4.2.1: OpenEye Scientific Software, Santa Fe, NM. <http://www.eyesopen.com.>,  
10 600 (n.d.).
- 11 601 44. B.P. Kelley, S.P. Brown, G.L. Warren, S.W. Muchmore, POSIT: flexible shape-guided  
12 602 docking for pose prediction, *J Chem Inf Model.* 55 (2015) 1771–1780.
- 13 603 45. M. McGann, FRED pose prediction and virtual screening accuracy, *J Chem Inf Model.* 51  
14 604 (2011) 578–596.
- 15 605 46. M. McGann, FRED and HYBRID docking performance on standardized datasets, *J*  
16 606 *Comput Aided Mol Des.* 26 (2012) 897–906.
- 17 607 47. P.C.D. Hawkins, A.G. Skillman, A. Nicholls, Comparison of shape-matching and docking  
18 608 as virtual screening tools, *J Med Chem.* 50 (2007) 74–82.
- 19 609 48. Abdallah IA, Hammad SF, Bedair A, Mansour FR. Sugaring-out induced homogeneous  
20 610 liquid-liquid microextraction as an alternative mode for biological sample preparation: A  
21 611 comparative study, *Journal of Separation Science.* 44 (2021):3117-25.
- 22 612 49. D. Devineni, D. Polidori, Clinical pharmacokinetic, pharmacodynamic, and drug–drug  
23 613 interaction profile of canagliflozin, a sodium-glucose co-transporter 2 inhibitor, *Clin*  
24 614 *Pharmacokinet.* 54 (2015) 1027–1041.
- 25 615 50. S. Kasichayanula, X. Liu, F. LaCreta, S.C. Griffen, D.W. Boulton, Clinical  
26 616 pharmacokinetics and pharmacodynamics of dapagliflozin, a selective inhibitor of sodium-glucose  
27 617 co-transporter type 2, *Clin Pharmacokinet.* 53 (2014) 17–27.
- 28 618 51. A.J. Scheen, Pharmacokinetic and pharmacodynamic profile of empagliflozin, a sodium  
29 619 glucose co-transporter 2 inhibitor, *Clin Pharmacokinet.* 53 (2014) 213–225.
- 30 620 52. K.A. Jacobson, Introduction to adenosine receptors as therapeutic targets, *Adenosine*  
31 621 *Receptors in Health and Disease.* (2009) 1–24.
- 32  
33  
34  
35  
36  
37  
38  
39  
40  
41  
42  
43  
44  
45  
46  
47  
48  
49  
50  
51  
52  
53  
54  
55  
56  
57  
58  
59  
60

1  
2  
3 623 53. M. Pastor-Anglada, S. Pérez-Torras, Who is who in adenosine transport, *Front Pharmacol.*  
4 624 9 (2018) 627.

5  
6 625 54. D. Zhang, W. Jin, H. Liu, T. Liang, Y. Peng, J. Zhang, Y. Zhang, ENT1 inhibition  
7 626 attenuates apoptosis by activation of cAMP/pCREB/Bcl2 pathway after MCAO in rats, *Exp*  
8 627 *Neurol.* 331 (2020) 113362.

9  
10  
11 628 55. J.B. Rose, Z. Naydenova, A. Bang, A. Ramadan, J. Klawitter, K. Schram, G. Sweeney, A.  
12 629 Grenz, H. Eltzhig, J. Hammond, Absence of equilibrative nucleoside transporter 1 in ENT1  
13 630 knockout mice leads to altered nucleoside levels following hypoxic challenge, *Life Sci.* 89 (2011)  
14 631 621–630.

15  
16 632

17  
18 633

19  
20 634

21  
22 635

23  
24 636

25  
26 637

27  
28 638

29  
30 639

31  
32 640

33  
34 641

35  
36 642

37  
38 643

39  
40 644

41  
42 645

43  
44 646

45  
46 647



648

**Figure legends**

<b>Figure</b>	<b>legend</b>
<b>(Figure 1)</b>	SGLTs effects and nephron distribution plus, CANA, DAPA, and EMPA chemical structures. (Made by www.BioRinder.com).
<b>(Figure 2)</b>	SGLT2 inhibitors similarity-based target fishing accompanied with docking results in (A&B) where's, (A) is representing the Highest score DAPA (magenta) plus ligand (green) interactions within hENT1, and (B) is representing Gliflozins (magenta) plus ligand (green) interactions within ENT1
<b>(Figure 3)</b>	LLOQ chromatograms obtained for CANA (1 µg/mL), DAPA (1 µg/mL), and EMPA (1 µg/mL), in plasma (P) and brain (B) samples.
<b>(Figure 4)</b>	(A) Formation of hydrogen bonds (dotted line) between the ligand and GLN 158 within pocket (B) Hydrogen bonds formation between DAPA and (ARG 345-ASN 407)

649

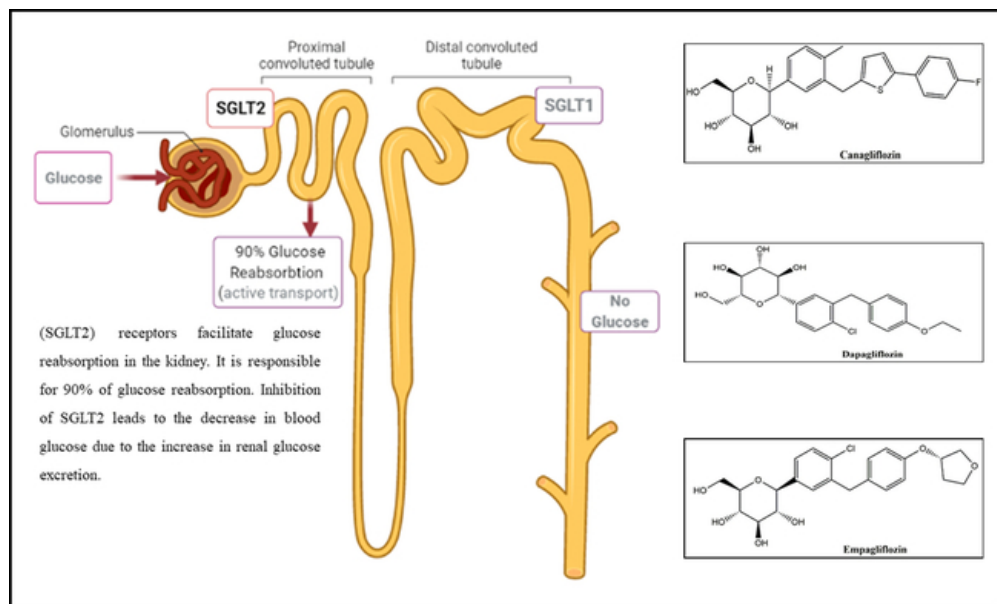


(Figure 1) SGLTs effects and nephron distribution plus, CANA, DAPA, and EMPA chemical structures. (Made by www.BioRinder.com).

27x16mm (600 x 600 DPI)

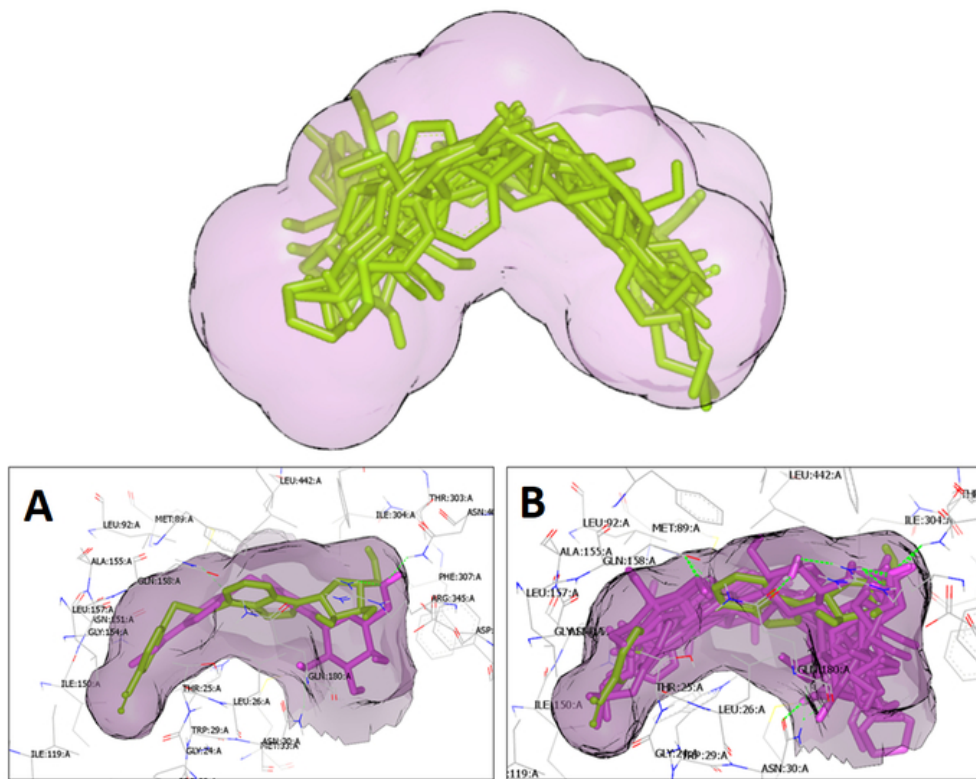


(Figure 2) SGLT2 inhibitors similarity-based target fishing accompanied with docking results in (A&B) where's, (A) is representing the Highest score DAPA (magenta) plus ligand (green) interactions within hENT1, and (B) is representing Gliflozins (magenta) plus ligand (green) interactions within ENT1

29x23mm (600 x 600 DPI)

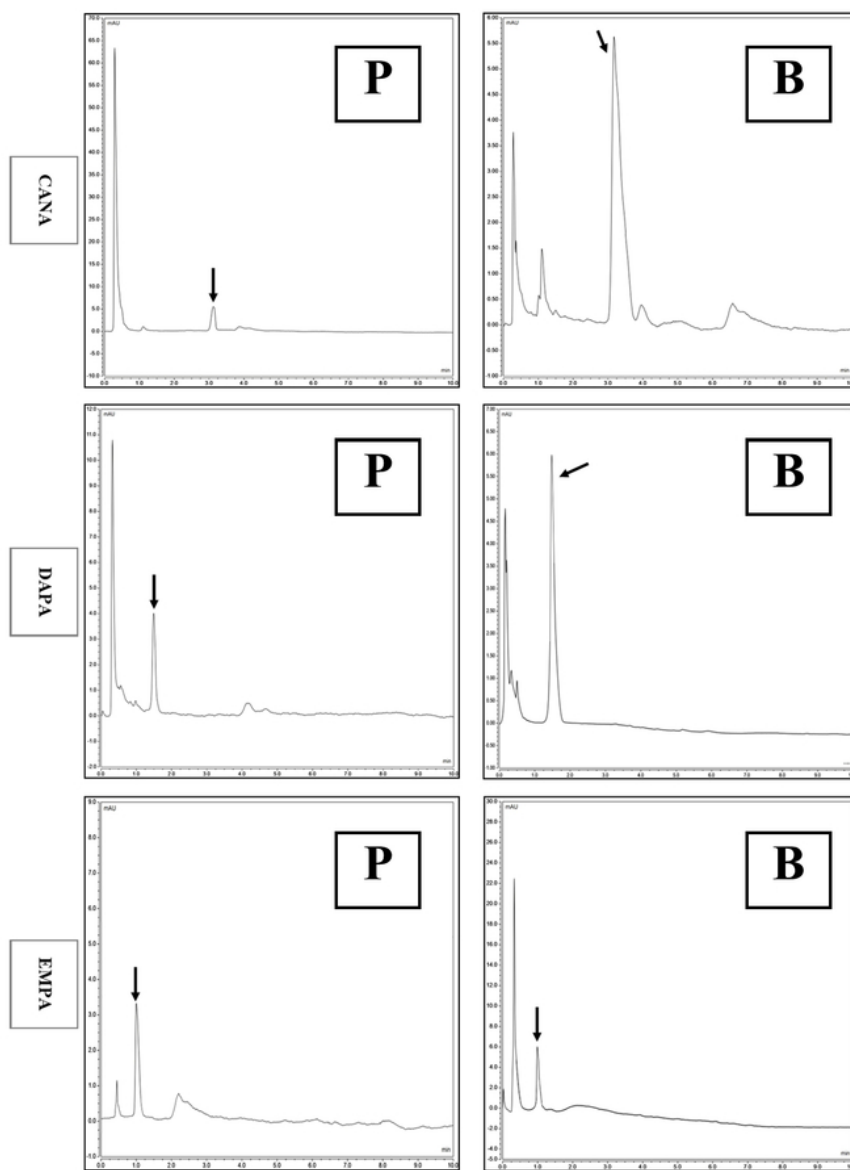


(Figure 3) LLOQ chromatograms obtained for CANA (1 µg/mL), DAPA (1 µg/mL), and EMPA (1 µg/mL), in plasma (P) and brain (B) samples.

28x38mm (600 x 600 DPI)

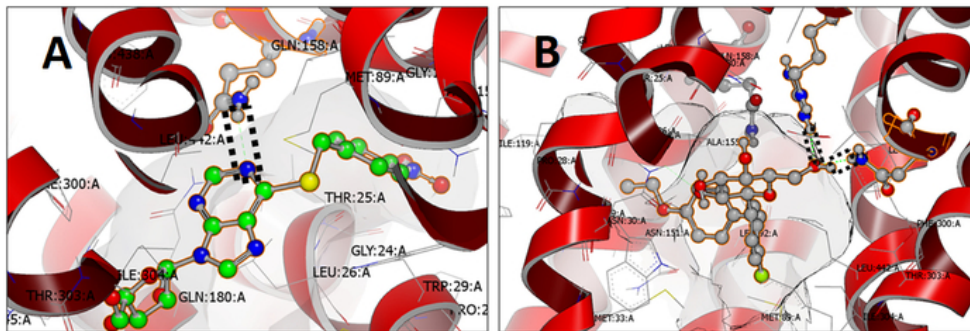


(Figure 4) (A) Formation of hydrogen bonds (dotted line) between the ligand and GLN 158 within pocket (B) Hydrogen bonds formation between DAPA and (ARG 345-ASN 407)

30x10mm (600 x 600 DPI)

**(Table 1)** Summary of the bioanalytical literature review for SGLT-2 inhibitors

	Author	Year	Matrix	Technique
<b>CANA</b>	<i>Iqbal et al.</i> [15]	2015	Rat Plasma	UHPLC-MS/MS
	<i>Iqbal et al.</i> [16]	2015	Human Plasma	HPLC-florescence detector
	<i>Dudhe et al.</i> [24]	2016	Human Plasma	HPLC-UV
	<i>Kobuchi et al.</i> [18]	2016	Rat Plasma	LC-MS/MS
	<i>Dong et al.</i> [19]	2018	Rat Plasma	UPLC-MS/MS
	<i>Mohamed et al.</i> [20]	2019	Human Plasma	LC-MS/MS
	<i>Ramisetti et al.</i> [21]	2019	Human Plasma	LC-MS/MS
	<i>Van Der Beek et al.</i> [22]	2020	Human Plasma & Urine	LC-MS/MS
	<i>Wattamwar et al.</i> [23]	2020	Human Plasma	LC-MS/MS
	<i>Alam et al.</i> [24]	2020	Human Plasma	HPTLC-UV
	<i>Emam et al.</i> [25]	2022	Human Plasma	HPTLC-UV
<b>DAPA</b>	<i>Aubry et al.</i> [26]	2010	Rat Plasma	LC-MS/MS
	<i>Goday et al.</i> [27]	2018	Human Plasma	LC-MS/MS
	<i>Donepudi et al.</i> [28]	2019	Human Plasma	HPLC-UV
	<i>Omar et al.</i> [29]	2019	Human Plasma	Spectro-fluorimetry
	<i>El-Zaher et al.</i> [30]	2019	Human Plasma	LC-MS/MS
	<i>Van Der Beek et al.</i> [22]	2020	Human Plasma	LC-MS/MS
	<i>Abbas et al.</i> [31]	2020	Rabbit Plasma	TLC-Spectrodensitometry
	<i>Abdel Gawad et al.</i> [32]	2021	Human Plasma	UPLC-UV
<b>EMPA</b>	<i>Donepudi et al.</i> [28]	2018	Human Plasma	HPLC-UV
	<i>Mabrouk et al.</i> [33]	2019	Human Plasma	HPLC-DAD
	<i>Shah et al.</i> [34]	2019	Human Plasma	LC-MS/MS
	<i>Wattamwar et al.</i> [23]	2020	Human Plasma	LC-MS/MS
	<i>Omar et al.</i> [29]	2020	Human Plasma	Spectro-fluorimetry
	<i>Rizk et al.</i> [35]	2020	Human Urine	Voltammetry
	<i>Van Der Beek et al.</i> [22]	2020	Human Plasma & Urine	LC-MS/MS

(Table 2) Precision, accuracy, extraction recovery, and matrix effect for CANA, DAPA and EMPA quality control samples.

Drug	Concentration µg/mL	Intraday precision		Inter-day precision		Matrix effect %	Extraction recovery %	
		CV %	Bias	CV %	Bias			
Rat's Plasma	CANA	3	4.94	-8.47	4.07	-4.34	81.25	80.23
		5	0.81	-5.69	4.65	-3.89	86.69	86.33
		8.5	0.49	1.96	1.15	2.83	97.55	94.48
	DAPA	3	1.39	-1.28	0.94	-2.63	80.42	85.75
		5	0.74	-1.31	0.66	-1.53	87.13	89.92
		8.5	1.41	0.59	1.79	1.67	91.73	92.98
	EMPA	3	1.37	-4.44	0.93	-4.56	68.89	65.03
		5	0.42	3.8	0.62	-3.5	87.28	88.84
		8.5	0.93	-1.35	0.65	-1.73	94.36	95.84
Rat's Brain	CANA	3	6.45	7.25	6.34	4.47	80.06	64.47
		5	0.57	-5.63	0.66	-5.08	84.32	69.34
		8.5	2.94	-2.93	0.73	-2.16	90.56	70.54
	DAPA	3	4.98	-13.37	2.24	-13.98	80.23	80.39
		5	5.53	-9.88	1.09	-11.67	86.19	85.29
		8.5	3.63	-8.99	3.12	-9.37	90.90	89.17
	EMPA	3	1.02	-8.81	1.84	-8.09	61.16	62.16
		5	0.81	-5.65	0.92	-5.46	77.56	83.31
		8.5	2.5	-3.61	1.87	-3.18	86.04	94.77

**(Table 3)** Gliflozins scores over ENT1 blind docking

Compounds	FRED Chemgauss4 score
<i>Dapagliflozin</i>	-14.5338
<i>Luseogliflozin</i>	-14.8904
<i>Canagliflozin</i>	-14.4942
<i>Sergliflozin etabonate</i>	-14.3366
<i>Ipragliflozin</i>	-14.3048
<i>Empagliflozin</i>	-13.595
<i>Ertugliflozin</i>	-13.2643
<i>Ligand</i>	-13.1777
<i>Tofogliflozin</i>	-13.0448
<i>Sotagliflozin</i>	-12.7628
<i>Remogliflozin</i>	-11.7353

hENT1 Docking

PDB ID [6OB6]